
Article:
Yang, X. orcid.org/0000-0001-6045-546X, Zhang, Y., Tang, H. orcid.org/0000-0002-2924-0126 et al. (4 more authors) (2025) Spring rapid temperature variability in Southern China: characteristics, decadal trend and associated climate impacts on crop yield. International Journal of Climatology. e8880. ISSN 0899-8418

https://doi.org/10.1002/joc.8880

Spring Rapid Temperature Variability in Southern China: Characteristics, Decadal Trend and Associated Climate Impacts on Crop Yield

Xianke Yang[1], Yixuan Zhang, Haosu Tang[3], Ping Huang[2], Xiaoxia Ling[1], Shaobing Peng[1], Dongliang Xiong[1]

Abstract

Climate-related risks are shaped not only by changes in mean temperatures, but also by temperature variability, which increases the probability of weather extremes and exerts profound impacts on society and ecosystems. Previous studies have documented contrasting seasonal trend differences in summer and winter temperature variability. However, spring temperature variability—a transitional period critical for agricultural production—has received limited attention. Using three indices, namely the standard deviation of daily temperature (STD), day-to-day temperature variability (DTD), and rapid cooling events (RCE), we analyze the decadal trends and drivers of spring temperature variability and quantify its effects on rice yield anomalies. Our findings reveal consistent trends in the spatial distribution of temperature variability, with increasing frequency and intensity in the Yangtze River Basin and Yunnan Province, and a decreasing trend across much of South China, closely following regional climatological patterns. Overall, the frequency and intensity of RCE trend exhibit a 'stronger getting weaker, weaker getting stronger' pattern, likely linked to increased STD trends driven by spatial non-uniformity of warming. Through a multiple regression statistical model, we find that climate factors, including mean climate and climate variability, explained 19%–49% of the variance in yield anomalies, with up to 11% of the explained variance attributable to spring temperature variability. This study underscores the critical role of spring temperature variability in climate resilience, informing strategies to enhance the adaptability of agricultural systems to extreme climate events.

1. Introduction

Climate change risks arise not only from growing mean temperatures but also from shifts in temperature variability (Olonscheck et al. 2021; Van Der Wiel and Bintanja 2021). It is well known that short-term temperature variability affects both human health and natural ecosystems. For instance, enhanced daily temperature variability has been associated with increased mortality rate (Healy et al. 2023; Pane and Davis 2024). Moreover, temperature variability modulates the frequency and intensity of extreme climate events, such as heat waves or droughts, exerting severe impacts on ecosystems and argricultrue (Ray et al. 2015; Vogel et al. 2019; Kotz et al. 2021; Lesk and Anderson 2021; Heinicke et al. 2022). While most existing studies have analyzed trends and impacts related to mean temperature changes (Alexander 2016; Li and Thompson 2021; Rezaei et al. 2023; Samset et al. 2023), the changes in short-term temperature variability, alongside the mechanisms driving these changes, have received comparatively limited attention. Understanding this variability is crucial for elucidating the long-term relationships between climate variability and extreme climate events, facilitating better-informed decision-making in climate change mitigation.

Previous studies on short-term temperature variability reveal significant seasonal differences. Reductions in temperature variability have been observed over high-northern latitudes in autumn (Screen 2014; Blackport et al. 2021) and mid-latitudes in winter (Schneider et al. 2015; Rhines et al. 2017), leading to fewer extreme cooling events in these seasons (Cui and He 2023; He et al. 2023). On the contrary, summer temperature variability has increased over most land areas, especially in Eurasia, southern China and tropical zones (Chan et al. 2020; Xu et al. 2020; Krauskopf and Huth 2024), exacerbating extreme heatwave events in recent decades (Schär et al. 2004; Perkins-Kirkpatrick and Gibson 2017; Wei et al. 2023). Climate model simulations also support these findings, revealing a decreasing trend in winter temperature variability and an increasing trend in summer temperature variability at mid-latitudes (Holmes et al. 2016; Bathiany et al. 2018; Tamarin-Brodsky et al. 2020). Mechanisms underlying these changes in temperature variability have been attributed to multiple physical processes, including meridional temperature gradients linked to Arctic amplification (Screen 2014; Bathiany et al. 2018; Dai and Deng 2021), soil moisture–temperature

feedbacks (Fischer et al. 2012), and local warming pattern (Chan et al. 2020; Tamarin-Brodsky et al. 2020).

However, insufficient attention has been paid to spring temperature variability. As a transitional season from cold to warm, spring plays a crucial role in agricultural production (Allstadt et al. 2015; Zhu et al. 2018). On one hand, it marks the harvest season for winter cereal crops in crop rotation systems (e.g., rapeseed-rice, winter wheat-rice); on the other hand, it serves as the sowing season for summer cereals (e.g., early rice, spring maize, spring wheat). Despite advancements in spring plant phenology under global warming, the risk of a 'false spring' is increasing (Allstadt et al. 2015; Chamberlain et al. 2019; Garner and Duran 2024). This phenomenon occurs when temperatures fluctuate rapidly from warm to cold anomalies, characterized by rapid cooling events and late spring cold spells (Xiao et al. 2018; Lin et al. 2023). Such rapid temperature variability can severely affect the growth, health, competitive ability, and geographical distribution limits of crops, ultimately leading to reduced crop yields. Previous studies revealed that climate factors account for more than one-third of the variations in global crop yield variability (Ray et al. 2015; Ray et al. 2019; Baffour-Ata et al. 2021), with 18%–43% of the explained variance attributable to climate extremes (Vogel et al. 2019). While it has been established that climate variability significantly affects crops during the growing season, the impact of rapid temperature variability in the special season remains underexplored.

As a major agricultural country, China is the world's largest producer of rice and wheat and the second-largest producer of maize, contributing 27%, 17%, and 24% of global production, respectively (FAO, 2023). The southern China is the core area for the rotational cropping system and the primary rice-growing region, where rice accounts for more than 70% of the national cultivation area (Figure 1a). Given the importance of southern China in food production, understanding the characteristics and impacts of climate variability in this region is crucial. However, relatively little attention has been paid to the transition season in the main grain-producing regions in the southern China. In particular, the decadal trends and impacts of spring temperature variability remain unclear, limiting comprehensive analyses of climate-related disaster impacts in this region.

In the present work, we aim to address the following questions through statistical analyses of long-term observations: 1) What are the observed changes in spring temperature variability, and 2) what mechanisms drive these changes? 3) To what extent does spring temperature variability affect crop production? Here, we present a comprehensive understanding of observed changes in spring temperature variability over the past half-century, identifying causal factors and quantifying the impact on crop yields. Our findings unveil a distinct pattern in the frequency and intensity of spring rapid cooling events, characterized by 'stronger getting weaker, weaker getting stronger'. This pattern is potentially related to the increased standard deviation trend caused by spatially uneven warming. Spring temperature variability can affect crop production through cold spells, precipitation, and gusty winds, explaining up to 8% of the variation in rice yields.

The rest of the paper is organized as follows. The datasets and methods are described in Section 2. Section 3 details the climatological distribution of rapid temperature variability. Section 4 explores decadal trends and underlying mechanisms of rapid temperature variability changes. Section 5 outlines effects of this variability on climate variations and crop yields. Finally, conclusion and discussion are given in Section 6.

2. Datasets and methods

2.1 Datasets

The climate variables used in this study were sourced from the National Meteorological Information Center of China Meteorological Administration, including daily minimum and mean temperature, precipitation, and wind data from 1961 to 2023 at over 2400 meteorological stations. The dataset has undergone rigorous quality control and homogenization and is widely used in the study of climate extremes in China (Cao et al. 2016; Han et al. 2024). To ensure consistency, stations with more than 30 days of missing data or relocations exceeding 100 meters were excluded, resulting in a selection of 587 stations in southern China (Figure 1b, colored dots).The selected stations encompass the majority of rice-growing regions and rotational cropping system areas in

China, spanning 13 provinces: Sichuan, Chongqing, Hubei, Anhui, Jiangsu, Guizhou, Henan, Jiangxi, Zhejiang, Yunnan, Guangxi, Guangdong and Fujian.

In addition, the yearly provincial rice planting areas and yields were obtained from the National Bureau of Statistics of China for the period of 1970–2022. Due to the inconsistency in the time span of the meteorological and yield data, the period from 1970 to 2022 was used to analyze the trend and effects of rapid temperature variability.

2.2 Definition of rapid temperature variability

Three methods are used here to quantify rapid temperature variability. Firstly, standard deviation of daily temperature (STD), calculated as the standard deviation of daily mean temperature, is a widely used meansure of rapid temperature variability (Blackport et al. 2021; Cui and He 2023; Krauskopf and Huth 2024). In addition, day-to-day temperature variability (DTD) is also used to meansure rapid temperature variability, which is defined as the absolute difference in daily temperatures between two adjacent days (Gough 2008; Xu et al. 2020; Ge et al. 2022), expressed as:

$$DTD = \frac{1}{n}\sum_{i=1}^{n} \mid \boldsymbol{T_{i+1}} - \boldsymbol{T_i} \mid$$

Where T_i denotes 2-meter temperature on day i, and n denotes the total days.

Although both STD and DTD can describe temperature variability, DTD is more representive than STD at describing the daily temperature change, particularly for distinguishing between orderly and oscillatory climates. For example, consider two daily temperature series: an orderly series (e.g., 25, 25, 25, 25, 15, 15, 15, 15 °C) and an oscillatory series (e.g., 25, 15, 25, 15, 25, 15, 25, 15 °C). Despite both having the same STD value (5.27 °C), they exhibit a significant difference in DTD (1.25 °C verus

8.75 °C). This makes DTD more effective at capturing rapid temperature variability in both orderly and oscillatory climate behaviors.

In addition to STD and DTD, rapid cooling event (RCE) was used to quantitatively characterize the frequency and intensity of daily temperature variability. Based on the absolute and relative thresholds, two types of definitions were used to identify RCE. For the relative threshold method, the day-to-day temperature difference (ΔT) was first calculated, and the relative threshold was defined as the 95th percentile from 1970 to 2022. Then, the RCE was identified when daily ΔT falls below the relative threshold. For the absolute threshold method, the RCE was selected as ΔT below -6 °C, which matches the threshold used in previous studies (Park et al. 2011; Cui and He 2023). More importantly, the mean relative threshold across the 836 stations in southern China is close to -6 °C. The frequency, mean intensity, and extreme intensity of RCE are calculated as:

$$Freqency_j = \sum_{i=1}^{M} \delta_{i,j}$$

$$Mean\ intensity_j = \frac{\sum_{i=1}^{M} \delta_{i,j} * \Delta T_{i,j}}{\sum_{i=1}^{M} \delta_{i,j}}$$

$$Extreme\ intensity_j = Min(\delta_{i,j} * \Delta T_{i,j})$$

Where δ is a symbolic function to judge RCE, in which $\delta_{i,j}$ = 1 for days with an RCE and $\delta_{i,j}$ = 0 for days without an RCE. i denotes the day in special seasons, and j denotes the year. $\sum()$ and $Min()$ indicate the sum and minimum value of the special seasons, repectively. Here, both the mean and extreme intensity are multiplied by -1 to express them as positive values for ease of interpretation.

2.3 Decadal trend and significant test

From the monthly and seasonal evolution of STD and DTD (Figure 2), it is clear that the temperature variability in southern China is strongest in spring, with March exhibiting significantly higher variability than other months. Meanwhile, given the importance of spring in agricultural production, the present study focused on the characteristics of spring temperature variability. The annual cycle of daily temperatures was removed before calculating STD, DTD and RCE.

To ensure reliable estimation of temperature variability using abundant samples, an 11-year sliding window was applied for calculating decadal trends. STD, DTD and RCE characteristics were calcaluted for each 11-year period (i.e. 1970–1980, 1972–1982, …, 2012–2022). Linear trend analysis was then used to calculate the decadal trend. All significant significance tests were conducted using a two-sided Student's t-test with a 0.05 (5%) critical level of significance.

2.4 Effect of spring variability on crop yield

To quantify the effect of spring variability on crop yield variability, a multi-parameter statistical model based on temperature and precipitation was constructed, using rice as an example. This approach has been widely used in previous studies (Ray et al. 2015; Ray et al. 2019; Vogel et al. 2019). Since the growth period of rice spans from March to November, the effects of climate variability in spring, summer, and autumn are considered here. At the provincial level, the detrended rice yield anomalies were linearly regressed against detrended climate anomalies, including mean temperature, temperature variability, mean precipitation and precipitation variability in spring, summer and autumn. The full statistical model is expressed as:

$$yield\ anomaly = \alpha_1 * Tmean_{MAM} + \alpha_2 * Tmean_{JJA} + \alpha_3 * Tmean_{SON} + \alpha_4 * Tstd_{MAM} + \alpha_5 * Tstd_{JJA} + \alpha_6 * Tstd_{SON} + \alpha_7 * Pmean_{MAM} + \alpha_8 * Pmean_{JJA} + \alpha_9 * Pmean_{SON} + \alpha_{10} * Pstd_{MAM} + \alpha_{11} * Pstd_{JJA} + \alpha_{12} * Pstd_{SON}$$

Where $Tmean$ and $Tstd$ denote the mean and standard deviation of temperature for the special seasons, respectively. Here, yield anomalies are defined as the raw yields minus a 9-year running mean, while climate variable anomalies are calculated by removing the anuual cycle from data with linear trends removed.

The overall R_2 of the equation represents the explained variance of climate variability on crop yield variability. A reduced statistical model was also constructed by removing $Tstd_{MAM}$ and $Pstd_{MAM}$ from the full model. The contribution of climate variability to crop yield was quantified by calculating the difference in R_2 between the full and reduced statistical models. In addition to the multi-parameter regression, ridge and lasso regressions were also used to quantify the effects of spring variablity, yielding similar results. Therefore, only the multi-parameter regression results are shown in this study.

3. Climatological distribution of rapid temperature variability

Figure 3 shows the climatology of STD and DTD in spring. The STD in southern China exhibits a zonal distribution, with high values exceeding 3.5 °C in Guizhou–Hunan–Jiangxi regions, and lower values located in the western parts of Yunnan and Sichuan (Figure 3a). This distribution contrasts significantly with the pattern of cold wave frequency in winter (Ma et al. 2022). There are notable differences in the monthly evolution of STD. Compared to April and May, the STD in March is generally higher and exhibits more pronounced spatial variability, with nearly 8% of stations exceeding 4.0 °C (Figure 3c), which is consisitent with Figure 2. In terms of monthly spatial distribution, the center of high values remains relatively stable over time and is consistently located in the Guizhou–Hunan–Jiangxi region (Figure S1). This region is the primary growing area for early rice cultivation, and as such, the risks associated with spring temperature variability, such as late spring cold spells, should be closely monitored and assessed in future agricultural planning and climate adaptation strategies.

As for DTD, its spatial distribution bears notable similarity to that of STD, with a spatial correlation coefficient exceeding 0.88 (Figure 3b). However, in contrast to STD, DTD remains relatively homogeneous from March to May, showing no significant monthly variation, especially with small spatial differences between March and April (Figure S1). Since STD is more sensitive to extreme values, the difference between STD and DTD suggests that more extreme events occur in March than in April and May, particularly rapid temperature change events.

Considering that STD and DTD alone cannot fully characterize extreme events in spring, Figure 4 illustrates the frequency, mean intensity, and extreme intensity of RCE using both relative and absolute threshold methods. The relative thresholds exhibit clear spatial heterogeneity, with high value centers located in the Guizhou–Hunan–Jiangxi, Anhui, and eastern Hubei. In these regions, only temperature drops exceeding -7°C can be ranked within the top 10% in history, indicating that historical temperature drops are notably larger here than those in surrounding areas. This distribution is consistent with the patterns observed in STD and DTD. Meanwhile, the mean instensity and extreme intensity in Figures 4b–c show similar spatial distributions with Figurer 4a, confirming that the spring temperature variability has the most severe impact on the Guizhou–Hunan–Jiangxi region.

For the absolute threshold method, an average threshold of -6°C, derived from the mean relative thresholds across all stations in Figure 4a (-5.98°C), was used to identify RCE. Despite differences in case selection methods, the spatial distributions of frequency, mean intensity, and extreme intensity of RCE (Figures 4d–f) remain generally consistent with those of the relative threshold method. Since both methods present consistent results in describing the characteristics of RCE, the absolute threshold method will be used in the subsequent section.

Regarding the monthly evolution, the spatial distribution of RCE frequency exhibits noticeable changes from March to May (Figure S2). The high-frequency center shifts

from the coastal region to the middle and lower reaches of the Yangtze River, accompanied by a slight decrease in RCE days. By May, the frequency substantially decreases across South China, except in the western Yunnan and Sichuan. This indicates that spring disasters related to temperature varability in southern China are mainly concentrated in early spring. As for the spatial distributions of mean and extreme intensity, they do not differ obviously from March to May.

Figures 3 and 4 show that the temperature variability calculated by STD and DTD aligns well with the distribution of RCE. To further establish their relationship, Figure 5 demonstrates the distribution of STD and RCE indices across 836 independent stations. It is evident that the relative threshold decreases linearly as STD increases, with the threshold dropping by 0.22 °C for each 0.1 °C rise in STD, suggesting a higher likelihood of frequent and intense RCEs in the region. Notably, the frequency and intensity of RCE also show a highly significant linear relationship with STD. Each 0.1°C rise in STD leads to an 11.2-day increase in frequency, as well as a 0.27°C and 0.29°C increase in mean and extreme intensity of RCE, respectively. Similar results are observed between DTD versus RCE (Figure S3). These findings establish a stable linear relationship between temperature variability and extreme events, especially for RCEs in spring. This implies that the frequency and intensity of RCE in a region can be estimated by straightforward calculations of STD or DTD in the future assessments.

Based on the above analysis on different aspects of rapid temperature variability, it can be concluded that, although three methods were used for definition, STD, DTD and RCE are robustly concentrated in the Guizhou–Hunan–Jiangxi region, with intensity weakening over time in climatology. Furthermore, the frequency and intensity of RCE can be effectively quantified by STD and DTD, providing a convenient method for characterizing extreme temperature events.

4. Decadal trends and causes for rapid temperature variability

To examine changes in rapid temperature variability, the decadal trend in RCE-related characteristics is shown in Figure 6. From 1970 to 2022, the frequency of RCE has increased in the Yangtze River Basin and Yunnan, with approximately 70% of the stations in Sichuan, Chongqing, Hubei, Anhui, Jiangsu, and Yunnan passing the 95% confidence level. The rates of increase in these provinces range from 0.1 to 1.8 days per decade. Conversely, a decreasing trend is observed in South China, particularly in Guizhou, Hunan, Jiangxi, Guangdong, Guangxi, Zhejiang, and Fujian, where rates range from -0.5 to -1.0 days per decade (Figure 6a). The spatial distribution of RCE frequency trend aligns well with its climatological pattern, that is, regions with higher climatological frequencies tend to exhibit a decreasing trend, while regions with lower climatological frequencies tend to show an increasing trend. It results in a distinct negative correlation between decadal changes and the climatological distribution, with a correlation coefficient reaching -0.34 for more than 800 independent samples (Figure 6d). These findings demonstrate that the decadal trend of RCE frequency follows a pattern of "stronger getting weaker, weaker getting stronger".

Similar results are observed for the mean and extreme intensity of RCE. Specifically, the mean intensity also demonstrates a decreasing trend in the Hunan–Jiangxi–Zhejiang region, consistent with its climatological distribution. Although the correlation between the climatological distribution and the mean intensity trend is modest at -0.11, it still passes the 99% confidence test due to the independence of each station's data. The decadal trend of extreme intensity is more pronounced, with a decreasing trend observed in Guizhou–Hunan–Jiangxi–Zhejiang. More than 64% of stations in these four provinces pass the 95% confidence test. Therefore, the decadal trend of extreme intensity corresponds better with the climatological distribution, with a correlation coefficient of -0.31. It indicates that regions with high mean-state extreme intensity tend to experience a weakening trend, and regions with weak mean-state extreme intensity tend to

295 experience a strengthening trend. Overall, these findings unveil a long-term trend pat-
296 tern in the frequency and intensity of RCE, characterized by a spatial distribution of
297 “stronger getting weaker, weaker getting stronger”.

298 To investigate the underlying mechanisms for the observed changes in RCE trends,
299 Figure 7 displays the corresponding trends in STD and DTD. Notably, the trend changes
300 in both STD and DTD share a similar spatial distribution with RCE, with a high spatial
301 correlation coefficient of 0.87. Specifically, both metrics demonstrate a downward trend
302 in South China, with over 70% of the stations in Guangxi, Guangdong, and Fujian pass-
303 ing the significance test. In the Yangtze River Basin and Yunnan Province, there is an
304 increasing trend, particularly in eastern Hubei, Anhui, and Jiangsu. This spatial distri-
305 bution closely aligns with the frequency of RCE, as evidenced by a robust linear rela-
306 tionship, indicated by a spatial correlation coefficient of 0.65. This suggests that the
307 observed trend changes in the frequency of RCE can largely be attributed to changes in
308 temperature variability. Specifically, an increase in temperature variability leads to a
309 rise in extreme events, subsequently elevating the frequency of RCEs. This is consistent
310 with the stable linear relationship depicted in Figure 5. Additionally, changes in DTD
311 trends can also help explain changes in RCE frequency (figure not shown).

312 To future unravel the possible drivers of the observed trends in temperature varia-
313 bility, Figure 8 presents the trend of mean temperature. It reveals that the warming rate
314 in South China is slower than in the Yangtze River Basin, with Guangxi, Guangdong,
315 and Fujian experiencing an average increase rate of 0.5–1.0°C per decade, considerably
316 lower than that of the Yangtze River Basin. Notably, the spatial pattern of mean tem-
317 perature trends closely matches those of STD and DTD. Regions with higher warming
318 rates correlate with increased STD, while areas with slower warming rates correspond
319 to decreased STD, yielding a correlation coefficient of 0.54. This finding suggests that
320 the observed changes in temperature variability trends are primarily driven by the spa-
321 tiotemporal heterogeneity in warming rates. This mechanism is in line with the

prevailing explanations (Chan et al. 2020; Tamarin-Brodsky et al. 2020), further emphasizing the role of local warming pattern in shaping regional temperature variability changes.

In summary, the trend analysis indicates that the frequency and intensity of RCE follow a spatial distribution characterized by "stronger getting weaker, weaker getting stronger". Specifically, there is a decreasing trend in South China and an increasing trend in the Yangtze River Basin and Yunnan. The changes in the frequency and intensity of RCE are mainly related to trend changes in STD and DTD, possibly driven by the spatial non-uniformity of warming.

5. Effects of variability on climate variations and crop yield

Spring temperature variability significantly affects agriculture and society by altering key climate variables. To quantify these impacts, Figure 9 illustrates the associated minimum temperature anomalies, precipitation, and wind speed during RCE. The analysis reveals that when RCEs occur, there is a 90% probability that the majority of stations will experience low temperatures, with minimum temperature anomalies dropping below 0°C (Figure 9a). The mean intensity of minimum temperature anomalies across provinces range from -1.0 to 6.4 °C, with notable high-value centers in the Guizhou–Hunan–Jiangxi region. Extreme minimum temperature anomalies can reach as low as -8 °C in Guizhou, Hunan, Jiangxi, Hubei, and Guangxi. This implies that RCEs are associated with severe cold weathers, potentially resulting in pronounced spring cold spells.

In addition to extreme cold temperature anomalies, RCEs are often accompanied by increased precipitation and gusty winds across most stations (Figures 9b–c). Specifically, the mean intensity of precipitation in southern China ranges from 5 to 18 mm/d, with high-value centers concentrated at the intersection of Hubei, Jiangxi, and Anhui. The extreme intensity of precipitation in these areas can reach up to 25 mm/d. Wind

speeds are similarly pronounced, with the highest recorded wind speed reaching 15 m/s in Jiangsu.

In terms of sub-seasonal evolution, there is no significant difference in the occurrence frequency of minimum temperature anomalies, precipitation, and winds, all with over 70% probability of occurrence during RCE (Figure 10). However, the intensity shows pronounced sub-seasonal variations. Minimum temperature anomalies and gusty winds are strongest in March and weaken as the month progresses. Precipitation, on the contrary, peaks in May with an average of 20 mm, more than twice the average in March, reflecting the sub-seasonal progression of the monsoon system in China (Ding and Chan 2005; Yang et al. 2023). These findings suggest that RCEs are accompanied by cold temperatures, precipitation and gusty winds, posing serious challenges for agricultural and broader social production.

To quantify the impact of spring RCE on crop yields, a statistical model was constructed to assess the relationship between yield anomalies and climate factors, using rice as an example. The climate factors include average anomalies of temperature and precipitation, as well as seasonal variability throughout the entire reproductive period of rice, totaling 12 elements. As depicted in Figure 11a, the explained variance of the statistical model across 13 provinces reveals that climate factors account for 19–49% of yield variability. Notably, Hubei and Guangdong contribute approximately 40%, while Sichuan shows a comparatively lower contribution. These findings align with previous results indicating that climate variability explains nearly one-third of the variability in crop yields (Ray et al. 2019; Vogel et al. 2019).

A reduced statistical model was constructed to quantify the contribution of spring temperature and precipitation variability by removing them from the 12 elements. The difference in the explained variance between the full and reduced statistical models is displayed in Figure 11b. The values across the 13 provinces range from 1%–11%, with a mean value of 4%. Higher values are observed in Yunan, Guizhou, Hunan, Hubei, and Anhui. This suggests that spring temperature variability and its associated climatic

impacts can account for roughly 4% of the variance in rice yield anomalies in southern China. In addition, the sensitivity to spring variability varies considerably from province to province, which may be related to local cropping systems, water and fertilizer management practices, and sowing varieties.

6. Conclusion and Discussion

This study explores the characteristics, trends and mechanisms of rapid temperature variability and quantifies its impact on crop yields. From various perspectives, rapid temperature variability is measured in terms of standard deviation of daily temperature (STD), day-to-day temperature variability (DTD) and rapid cooling event (RCE). These indices show a consistent climatological pattern for spring temperature variability, with greater variability and more frequent and stronger RCEs observed in the Guizhou–Hunan–Jiangxi region. Despite differences in calculation methods, the frequency and intensity of RCEs exhibit strong linear relationships with both STD and DTD. Specifically, an increase of 0.1°C in STD correlates with an 11.2-day increase in RCE frequency, alongside increases of 0.27°C and 0.29°C in mean and extreme intensity, respectively. Thus, temperature variability serves as a reliable indicator of RCE characteristics.

Over the past half century, the spatial distribution of long-term trends in rapid temperature variability across southern China reveals significant heterogeneity. Specifically, RCEs have become more frequent and intense in the Yangtze River Basin and Yunnan. Over these provinces, the frequency of RCEs in spring has increased by 0.1 to 1.8 days per decade, while the extreme intensity of RCEs has grown by 0.9 to 2.7 °C per decade. Conversely, the frequency and intensity of RCEs exhibit a negative trend across most of South China. This trend pattern aligns with the overall climatological distribution, following a ‘stronger getting weaker, weaker getting stronger’ pattern. The observed trends in RCEs are mainly related to the trend changes in STD and DTD, which is driven by spatial non-uniformity in warming. This finding highlights an important consideration that although global warming has enabled the possibility of earlier rice sowing (Olesen et al. 2012; Fatima et al. 2020; Minoli et al. 2022), the increased variability in spring temperatures introduces a heightened risk for

crop failure. Therefore, the spring temperature variability deserves more attention in agricultural production.

Rapid temperature variability has profound implications for both agriculture and society by altering key climate variables. RCEs are frequently accompanied by low temperatures, precipitation, and gusty winds, which can severely impact agricultural productivity and social stability. Our statistical model demonstrates that climate factors, including mean climate as well as climate variability—explain 19%–49% of the variance in rice yield anomalies. Although the quantified contributions are not directly comparable across studies due to differences in regional contexts and methodologies, the influence of climate factors on yield variability is consistent with previous findings, which suggested that climate factors explain approximately one-third of crop yield variations (Ray et al. 2015).

Moreover, we demonstrate that spring variability associated with climate extremes contributes up to 11% of the explained variance in rice yield anomalies. This contribution is lower than the 26% attributed to climate variability in a previous study (Vogel et al. 2019), likely because this study focuses specifically on spring rather than full-season variability. Our results also indicate that summer variability contributes more significantly than spring and autumn variability (results not shown), which may be due to the greater sensitivity of rice to extreme heat waves and heat stress during the flowering and filling periods (Wang et al. 2019; Song et al. 2022). Additionally, this study centers on local regions rather than national or global scales, recognizing that the influence of climate variability on yield variability can differ substantially across regions due to disparities in agricultural practices, climatic conditions, and crop management (Heino et al. 2018; Anderson et al. 2019; Lesk et al. 2022). To build on this work, future research could broaden the geographic scope to encompass diverse regions and agricultural systems, which would provide a more comprehensive understanding of climate impacts on crops. Additionally, exploring the dynamic mechanisms of changes in temperature variability and crop responses through general circulation model simulations will be crucial. Such approaches can enhance predictive ability, helping to inform region-specific adaptation strategies and increase agricultural resilience to climate extremes.

Acknowledgements

This work was supported by the Natural Science Foundation of Hubei Province, China (Program No. 2024AFB115) and the Fundamental Research Funds for the Central Universities (Program No. 2662024ZKQD003).

Data Availability

The meteorological station data is available at https://data.cma.cn. The yield and area data are freely available at https://data.stats.gov.cn/easyquery.htm?cn=E0103. The analysis scripts are available upon request from the corresponding author.

Reference:

Alexander, L. V., 2016: Global observed long-term changes in temperature and precipitation extremes: A review of progress and limitations in ipcc assessments and beyond. *Weather Clim. Extreme.*, **11**, 4-16, https://doi.org/10.1016/j.wace.2015.10.007.

Allstadt, A. J., S. J. Vavrus, P. J. Heglund, A. M. Pidgeon, W. E. Thogmartin, and V. C. Radeloff, 2015: Spring plant phenology and false springs in the conterminous us during the 21st century. *Environ. Res. Lett.*, **10**, 104008, https://doi.org/10.1088/1748-9326/10/10/104008.

ANDERSON, W. B., R. SEAGER, W. BAETHGEN, M. CANE, and L. YOU, 2019: Synchronous crop failures and climate-forced production variability. *Sci. Adv.*, **5**, https://doi.org/10.1126/sciadv.aaw1976.

Baffour-Ata, F., P. Antwi-Agyei, E. Nkiaka, A. J. Dougill, A. K. Anning, and S. O. Kwakye, 2021: Effect of climate variability on yields of selected staple food crops in northern ghana. *J. Agr. Food Res.*, **6**, 100205, https://doi.org/10.1016/j.jafr.2021.100205.

Bathiany, S., V. Dakos, M. Scheffer, and T. M. Lenton, 2018: Climate models predict increasing temperature variability in poor countries. *Sci. Adv.*, **4**, eaar5809, https://doi.org/10.1126/sciadv.aar5809.

Blackport, R., J. C. Fyfe, and J. A. Screen, 2021: Decreasing subseasonal temperature variability in the northern extratropics attributed to human influence. *Nat. Geosci.*, **14**, 719-723, https://doi.org/10.1038/s41561-021-00826-w.

Cao, L., Y. Zhu, G. Tang, F. Yuan, and Z. Yan, 2016: Climatic warming in China according to a homogenized data set from 2419 stations: Climatic warming in china. *Int. J. Climatol.*, **36**, 4384-4392, https://doi.org/10.1002/joc.4639.

Chamberlain, C. J., B. I. Cook, I. García De Cortázar-Atauri, and E. M. Wolkovich, 2019: Rethinking false spring risk. *Global Change Biol.*, **25**, 2209-2220, https://doi.org/10.1111/gcb.14642.

476 Chan, D., A. Cobb, L. R. V. Zeppetello, D. S. Battisti, and P. Huybers, 2020:
477 Summertime temperature variability increases with local warming in
478 midlatitude regions. *Geophys. Res. Lett.*, **47**, e2020GL087624,
479 https://doi.org/10.1029/2020GL087624.
480 Cui, Z., and C. He, 2023: Decadal trend of synoptic temperature variability over the
481 northern hemisphere in winter. *Theor. Appl. Climatol.*, **152**, 829-842,
482 https://doi.org/10.1007/s00704-023-04423-2.
483 Dai, A., and J. Deng, 2021: Arctic amplification weakens the variability of daily
484 temperatures over northern middle-high latitudes. *J. Climate*, **34**, 2591-2609,
485 https://doi.org/10.1175/JCLI-D-20-0514.1.
486 Ding, Y., and J. C. L. Chan, 2005: The East Asian summer monsoon: An overview.
487 *Meteor. Atmos. Phys.*, **89**, 117–142, https://doi.org/10.1007/s00703-005-0125-z.
488 Fatima, Z., and et al. , 2020: The fingerprints of climate warming on cereal crops
489 phenology and adaptation options. *Sci. Rep.*, **10**,
490 https://doi.org/10.1038/s41598-020-74740-3.
491 Fischer, E. M., J. Rajczak, and C. Schär, 2012: Changes in european summer
492 temperature variability revisited. *Geophys. Res. Lett.*, **39**, L19702,
493 https://doi.org/10.1029/2012GL052730.
494 Garner, A. J., and D. P. Duran, 2024: Late-winter and springtime temperature variations
495 throughout new jersey in a warming climate. *J. Appl. Meteorol. Clim.*, **63**, 197-
496 207, https://doi.org/10.1175/JAMC-D-23-0152.1.
497 Ge, J., Q. Liu, B. Zan, Z. Lin, S. Lu, B. Qiu, and W. Guo, 2022: Deforestation intensifies
498 daily temperature variability in the northern extratropics. *Nat. Commun.*, **13**,
499 5955, https://doi.org/10.1038/s41467-022-33622-0.
500 Gough, W. A., 2008: Theoretical considerations of day-to-day temperature variability
501 applied to toronto and calgary, canada data. *Theor. Appl. Climatol.*, **94**, 97-105,
502 https://doi.org/10.1007/s00704-007-0346-9.

Han, J., S. Fang, X. Wang, W. Zhuo, Y. Yu, X. Peng, and Y. Zhang, 2024: The impact of intra-annual temperature fluctuations on agricultural temperature extreme events and attribution analysis in mainland China. *Sci. Total Environ.*, **949**, 174904, https://doi.org/10.1016/j.scitotenv.2024.174904.

He, Y., X. Wang, B. Zhang, Z. Wang, and S. Wang, 2023: Contrast responses of strong and weak winter extreme cold events in the northern hemisphere to global warming. *Climate Dyn.*, **61**, 4533-4550, https://doi.org/10.1007/s00382-023-06822-7.

Healy, J. P., and et al. , 2023: Seasonal temperature variability and mortality in the medicare population. *Environ. Health Persp.*, **131**, 077002, https://doi.org/10.1289/EHP11588.

Heinicke, S., K. Frieler, J. Jägermeyr, and M. Mengel, 2022: Global gridded crop models underestimate yield responses to droughts and heatwaves. *Environ. Res. Lett.*, **17**, 044026, https://doi.org/10.1088/1748-9326/ac592e.

Heino, M., M. J. Puma, P. J. Ward, D. Gerten, V. Heck, S. Siebert, and M. Kummu, 2018: Two-thirds of global cropland area impacted by climate oscillations. *Nat Commun*, **9**, 1257, https://doi.org/10.1038/s41467-017-02071-5.

Holmes, C. R., T. Woollings, E. Hawkins, and H. De Vries, 2016: Robust future changes in temperature variability under greenhouse gas forcing and the relationship with thermal advection. *J. Climate*, **29**, 2221-2236, https://doi.org/10.1175/JCLI-D-14-00735.1.

Kotz, M., L. Wenz, A. Stechemesser, M. Kalkuhl, and A. Levermann, 2021: Day-to-day temperature variability reduces economic growth. *Nat. Climate Change*, **11**, 319-325, https://doi.org/10.1038/s41558-020-00985-5.

Krauskopf, T., and R. Huth, 2024: Trends in intraseasonal temperature variability in europe: Comparison of station data with gridded data and reanalyses. *Int. J. Climatol.*, **44**, 3054-3074, https://doi.org/10.1002/joc.8512.

Lesk, C., and W. Anderson, 2021: Decadal variability modulates trends in concurrent heat and drought over global croplands. *Environ. Res. Lett.*, **16**, 055024, https://doi.org/10.1088/1748-9326/abeb35.

Lesk, C., and et al. , 2022: Compound heat and moisture extreme impacts on global crop yields under climate change. *Nat. Rev. Earth Env.*, **3**, 872-889, https://doi.org/10.1038/s43017-022-00368-8.

Li, J., and D. W. J. Thompson, 2021: Widespread changes in surface temperature persistence under climate change. *Nature*, **599**, 425-430, https://doi.org/10.1038/s41586-021-03943-z.

Lin, F., and et al. , 2023: Late spring cold reduces grain number at various spike positions by regulating spike growth and assimilate distribution in winter wheat. *Crop J.*, **11**, 1272-1278, https://doi.org/10.1016/j.cj.2023.03.014.

Ma, L., Z. Wei, and X. Li, 2022: Spatial and temporal characteristics of various cold surges over China during 1962–2018. *Int. J. Climatol.*, **42**, 10253-10267, https://doi.org/10.1002/joc.7896.

Minoli, S., J. Jägermeyr, S. Asseng, A. Urfels, and C. Müller, 2022: Global crop yields can be lifted by timely adaptation of growing periods to climate change. *Nat. Commun.*, **13**, https://doi.org/10.1038/s41467-022-34411-5.

Olesen, J. E., and et al. , 2012: Changes in time of sowing, flowering and maturity of cereals in europe under climate change. *Food Additives and Contaminants Part a-Chemistry Analysis Control Exposure & Risk Assessment*, **29**, 1527-1542, https://doi.org/10.1080/19440049.2012.712060.

Olonscheck, D., A. P. Schurer, L. Lücke, and G. C. Hegerl, 2021: Large-scale emergence of regional changes in year-to-year temperature variability by the end of the 21st century. *Nat. Commun.*, **12**, 7237, https://doi.org/10.1038/s41467-021-27515-x.

Pane, M. M., and R. E. Davis, 2024: The association between short-term temperature variability and mortality in virginia. *PLOS ONE*, **19**, e0310545, https://doi.org/10.1371/journal.pone.0310545.

Park, T.-W., C.-H. Ho, S.-J. Jeong, Y.-S. Choi, S. K. Park, and C.-K. Song, 2011: Different characteristics of cold day and cold surge frequency over East Asia in a global warming situation. *J. Geophys. Res.*, **116**, D12118, https://doi.org/10.1029/2010JD015369.

Perkins-Kirkpatrick, S. E., and P. B. Gibson, 2017: Changes in regional heatwave characteristics as a function of increasing global temperature. *Sci. Rep.*, **7**, 12256, https://doi.org/10.1038/s41598-017-12520-2.

Ray, D. K., J. S. Gerber, G. K. MacDonald, and P. C. West, 2015: Climate variation explains a third of global crop yield variability. *Nat. Commun.*, **6**, 5989, https://doi.org/10.1038/ncomms6989.

Ray, D. K., P. C. West, M. Clark, J. S. Gerber, A. V. Prishchepov, and S. Chatterjee, 2019: Climate change has likely already affected global food production. *Plos One*, **14**, e0217148, https://doi.org/10.1371/journal.pone.0217148.

Rezaei, E. E., and et al. , 2023: Climate change impacts on crop yields. *Nat. Rev. Earth Env.*, **4**, 831-846, https://doi.org/10.1038/s43017-023-00491-0.

Rhines, A., K. A. McKinnon, M. P. Tingley, and P. Huybers, 2017: Seasonally resolved distributional trends of North american temperatures show contraction of winter variability. *J. Climate*, **30**, 1139-1157, https://doi.org/10.1175/JCLI-D-16-0363.1.

Samset, B. H., C. Zhou, J. S. Fuglestvedt, M. T. Lund, J. Marotzke, and M. D. Zelinka, 2023: Steady global surface warming from 1973 to 2022 but increased warming rate after 1990. *Commun. Earth Environ.*, **4**, 400, https://doi.org/10.1038/s43247-023-01061-4.

582 Schär, C., P. L. Vidale, D. Lüthi, C. Frei, C. Häberli, M. A. Liniger, and C. Appenzeller,
583 2004: The role of increasing temperature variability in european summer
584 heatwaves. *Nature*, **427**, 332-336, https://doi.org/10.1038/nature02300.
585 Schneider, T., T. Bischoff, and H. Płotka, 2015: Physics of changes in synoptic
586 midlatitude temperature variability. *J. Climate*, **28**, 2312-2331,
587 https://doi.org/10.1175/JCLI-D-14-00632.1.
588 Screen, J. A., 2014: Arctic amplification decreases temperature variance in northern
589 mid- to high-latitudes. *Nat. Climate Change*, **4**, 577-582,
590 https://doi.org/10.1038/nclimate2268.
591 Song, Y. L., and et al. , 2022: The negative impact of increasing temperatures on rice
592 yields in southern China. *Sci. Total Environ.*, **820**,
593 https://doi.org/10.1016/j.scitotenv.2022.153262.
594 Tamarin-Brodsky, T., K. Hodges, B. J. Hoskins, and T. G. Shepherd, 2020: Changes in
595 northern hemisphere temperature variability shaped by regional warming
596 patterns. *Nat. Geosci.*, **13**, 414-421, https://doi.org/10.1038/s41561-020-0576-
597 3.
598 Van Der Wiel, K., and R. Bintanja, 2021: Contribution of climatic changes in mean and
599 variability to monthly temperature and precipitation extremes. *Commun. Earth*
600 *Environ.*, **2**, 1, https://doi.org/10.1038/s43247-020-00077-4.
601 Vogel, E., and et al. , 2019: The effects of climate extremes on global agricultural yields.
602 *Environ. Res. Lett.*, **14**, 054010, https://doi.org/10.1088/1748-9326/ab154b.
603 Wang, Y. L., and et al. , 2019: Research progress on heat stress of rice at flowering stage.
604 *Rice Science*, **26**, 1-10, https://doi.org/10.1016/j.rsci.2018.06.009.
605 Wei, J., W. Q. Han, W. G. Wang, L. Zhang, and B. Rajagopalan, 2023: Intensification
606 of heatwaves in China in recent decades: Roles of climate modes. *Npj Clim.*
607 *Atmos. Sci.*, **6**, 98, https://doi.org/10.1038/s41612-023-00428-w.

608 Xiao, L., and et al. , 2018: Estimating spring frost and its impact on yield across winter
609 wheat in China. *Agr. Forest Meteorol.*, **260-261**, 154-164,
610 https://doi.org/10.1016/j.agrformet.2018.06.006.
611 Xu, Z., F. Huang, Q. Liu, and C. Fu, 2020: Global pattern of historical and future
612 changes in rapid temperature variability. *Environ. Res. Lett.*, **15**, 124073,
613 https://doi.org/10.1088/1748-9326/abccf3.
614 Yang, X., P. Huang, P. Hu, and Z. Wang, 2023: Distinct impacts of two types of summer
615 ENSO with different temporal evolutions on the Asian summer monsoon: Role
616 of the tropical Indo-western Pacific. *J. Climate*, **36**, 3917–3936,
617 https://doi.org/10.1175/JCLI-D-22-0532.1.
618 Zhu, Y.-L., H.-J. Wang, T. Wang, and D. Guo, 2018: Extreme spring cold spells in North
619 China during 1961–2014 and the evolving processes. *Atmos. Ocean. Sci. lett.*,
620 **11**, 432-437, https://doi.org/10.1080/16742834.2018.1514937.
621
622

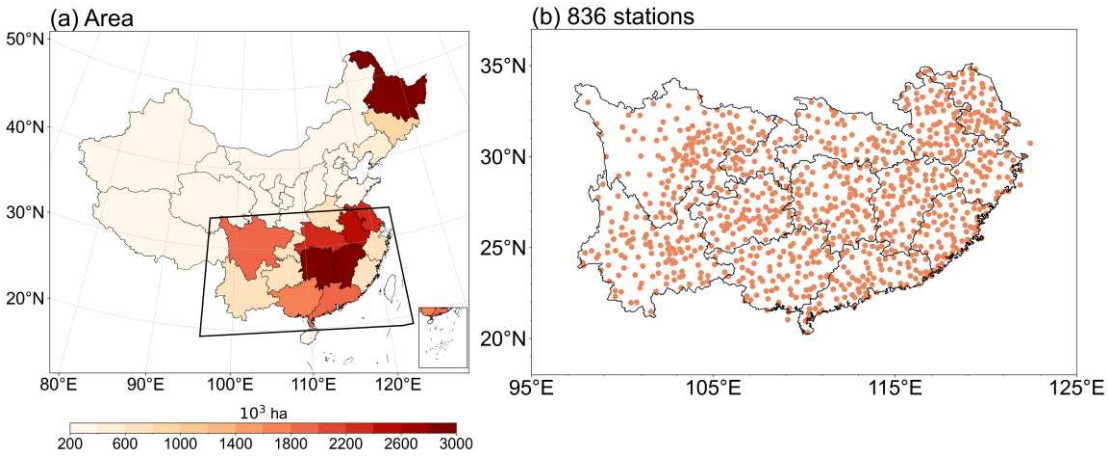

Figure1 The study area in southern China. (a) Spatial distribution of average rice planting area in recent five years. The black box in (a) represents the southern China domain. (b) Distribution of 725 meteorological stations in southern China.

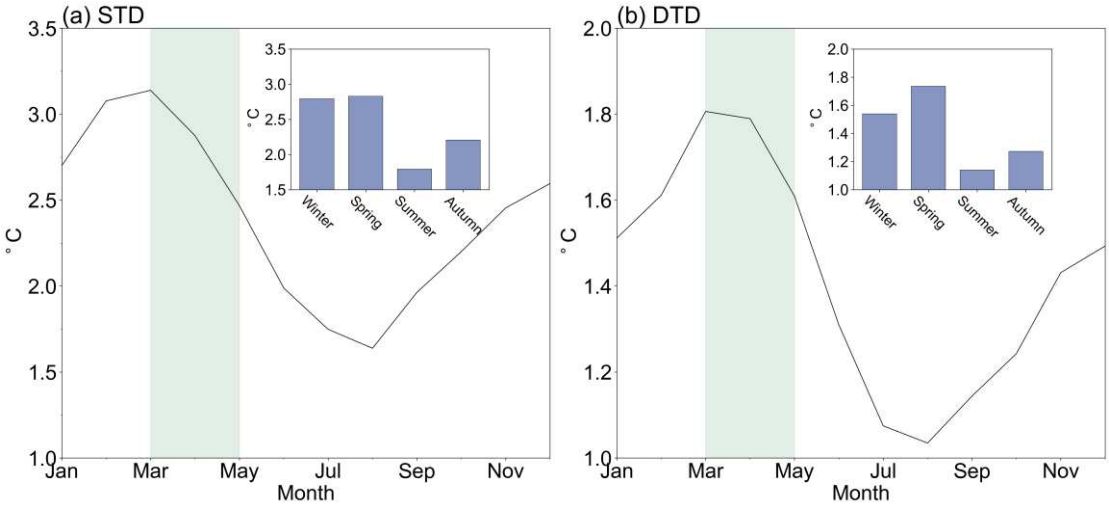

Figure 1 Monthly and seasonal evolution of temperature variability. (a) The black line indicates the multi-year monthly standard deviation of daily temperature from 1970 to 2022. The bar chart represents the multi-year seasonal standard deviation. The light-grey shade indicates March to May. (b) as in (a), but for DTD.

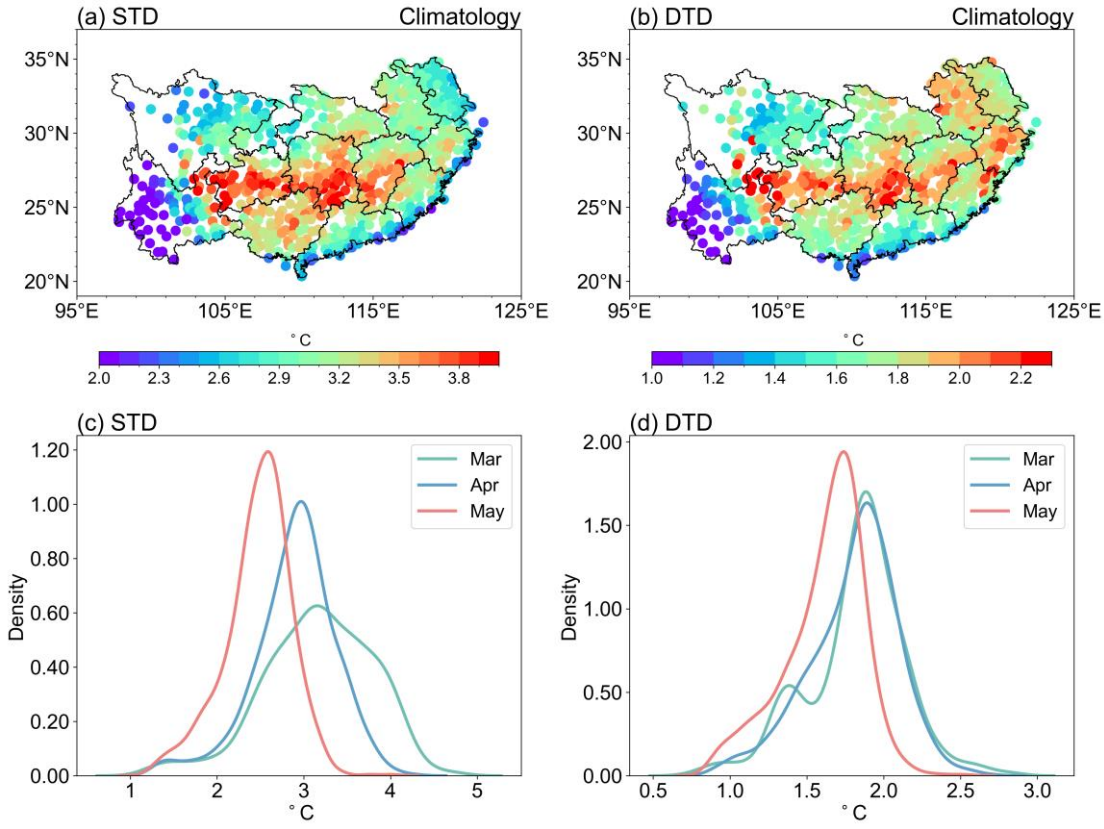

635

636 **Figure 3 Climatology of STD and DTD.** Spring mean (a) STD and (b) DTD of daily
637 temperature in southern China from 1970 to 2022. Probability density functions of
638 monthly (c) STD and (d) DTD fitted by kernel density estimation for 836 meteorolog-
639 ical stations in southern China.

640

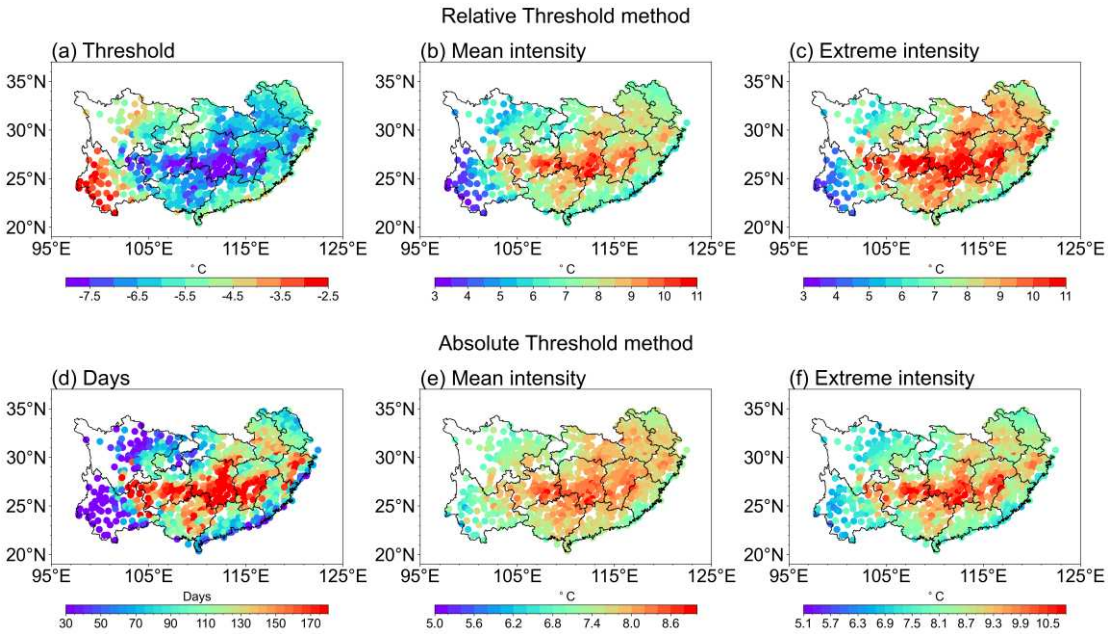

641

642 **Figure 4 Characteristics of rapid cooling events**. Spatial distribution of (a) relative
643 threshold, and seasonal means of (b) mean intensity as well as (c) extreme intensity of
644 RCE from 1970 to 2022 based on the relative threshold method. (d–f) as in (a–c), but
645 for days, mean intensity and extreme intensity based on the absolute threshold method.

646

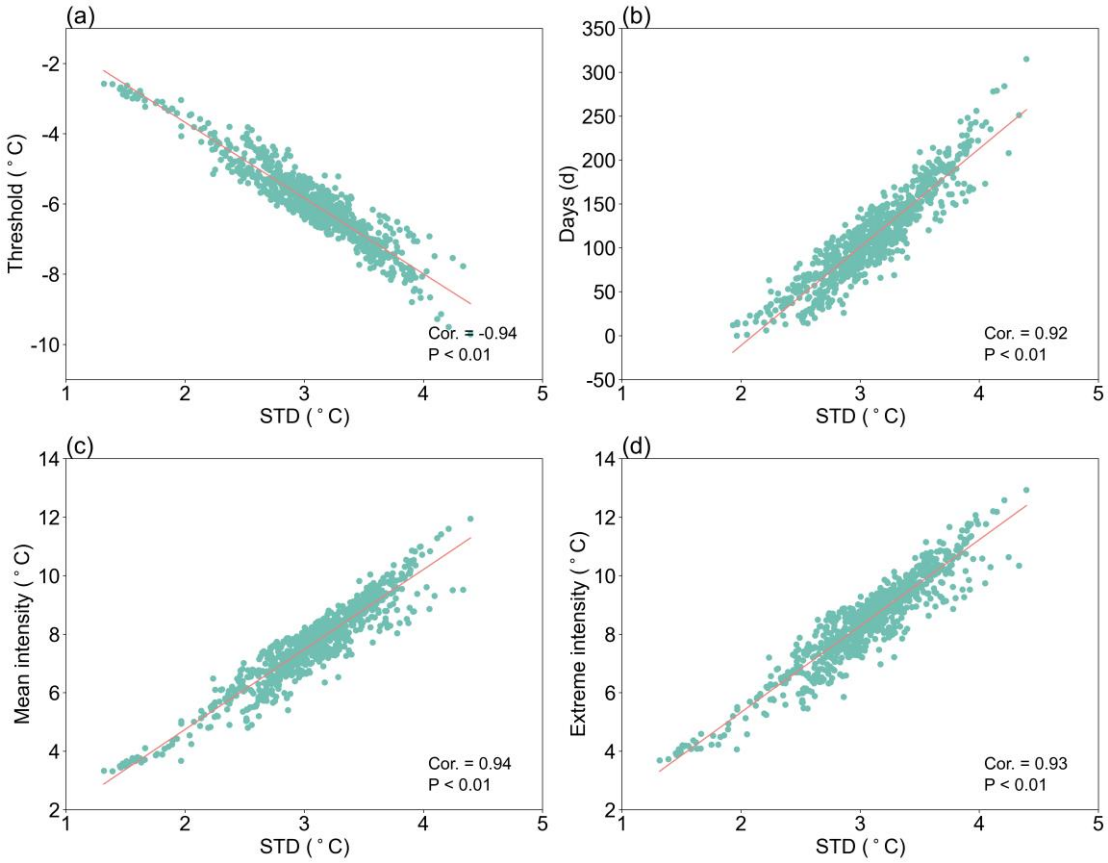

647

648 **Figure 5 Relationship between STD and RCE**. Scatter plots for regional averaged
649 spring STD and (a) threshold, (b) days, (c) mean intensity and (d) extreme intensity of
650 RCE from 1970 to 2022 across 836 meteorological stations in southern China. The
651 leastsquares fitting line is shown as the black line in each panel. Correlation coefficients
652 and p-value are labelled in the lower left of each panel.

653

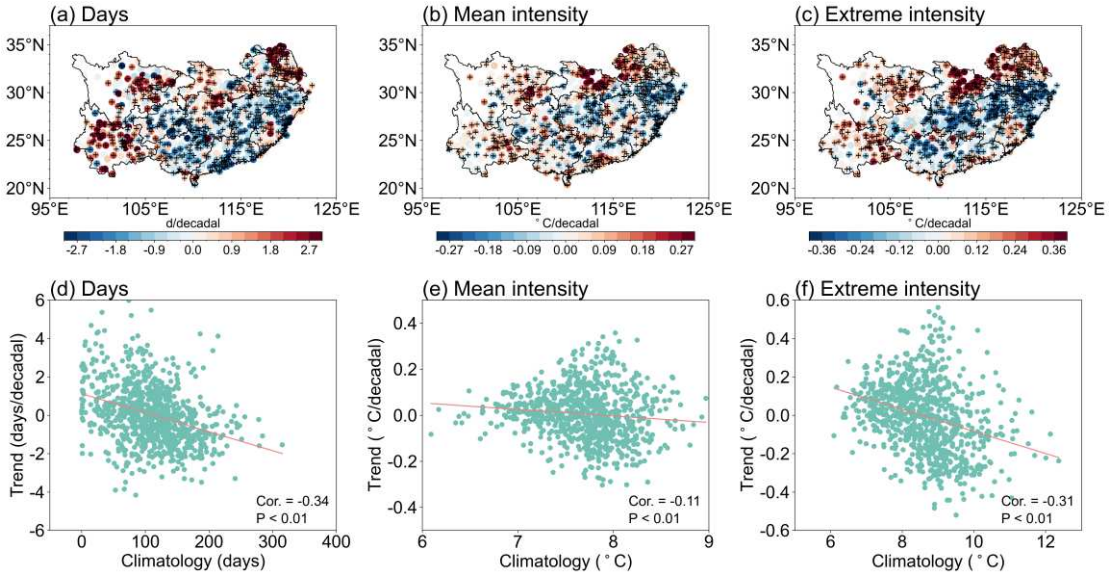

654

655 **Figure 6 Decadal trend of characteristics related to RCE.** The decadal trend of (a)
656 days, (b) mean intensity, (c) extreme intensity of RCE from 1970 to 2022. A plus sign
657 denotes statistical significance exceeding the 95% confidence level. The relationship
658 between trend in (d) days, (e) mean intensity, (f) extreme intensity and their climatology
659 for 836 meteorological stations. The least squares fitting line is shown as the black line
660 in each panel. Correlation coefficients and p-value are labelled in the lower right of
661 each panel.

662

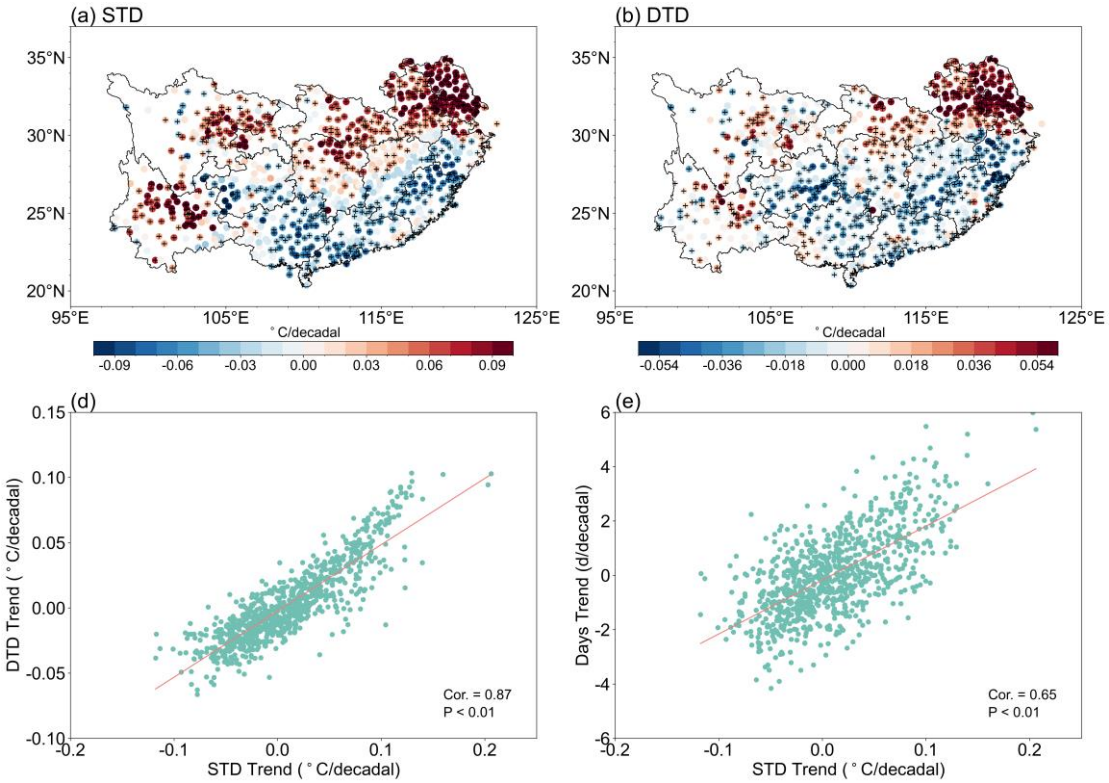

Figure 7 Decadal trend of STD and DTD. (a, b) as in Figure 6 (a, b, c), but for the results of STD and DTD. (c, d) as in Figure 6 (d, e, f), but for the relationship between (c) STD trend and DTD trend, and (d) STD trend and day trend for 836 meteorological stations.

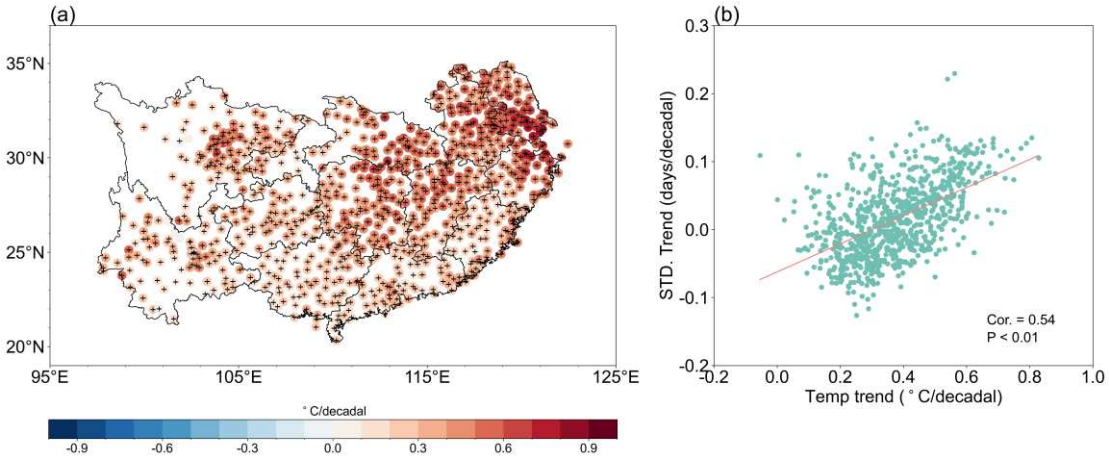

Figure 8 Decadal trend of mean temperature. (a) as in Figure 6 (a), but for the results of spring mean temperature. (b) as in Figure 6 (d), but for the relationship between STD trend and mean temperature trend.

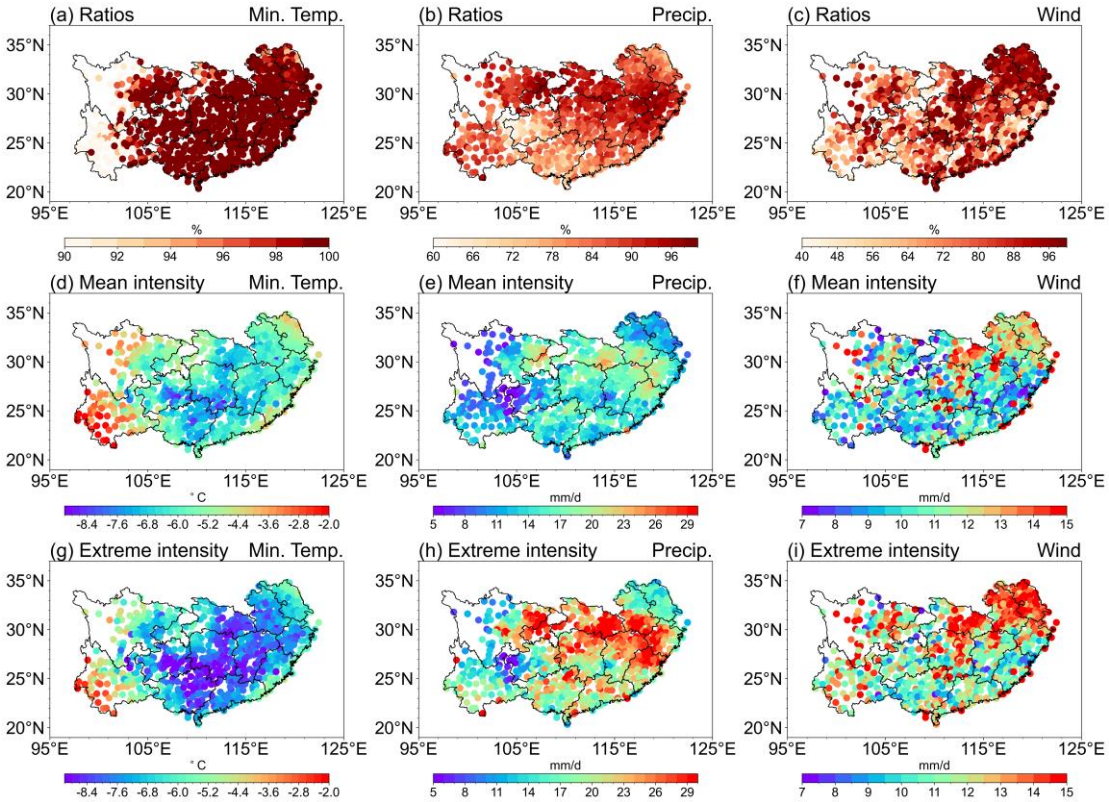

673

674 **Figure 9 Characteristics of climate variables related to RCE**. Spatial distribution
675 of (a) frequency ratio, (d) mean intensity and (g) extreme intensity of minimum tem-
676 peratures anomalies below 0°C during RCE from 1970 to 2022. Anomalies are calcu-
677 lated with annual cycle removed. (b, e, h) as in (a, d, g), but for results with precipitation
678 exceeding 1 mm/d. (c, f, i) as in (a, d, g), but for results with wind speed exceeding 7
679 m/s.

680

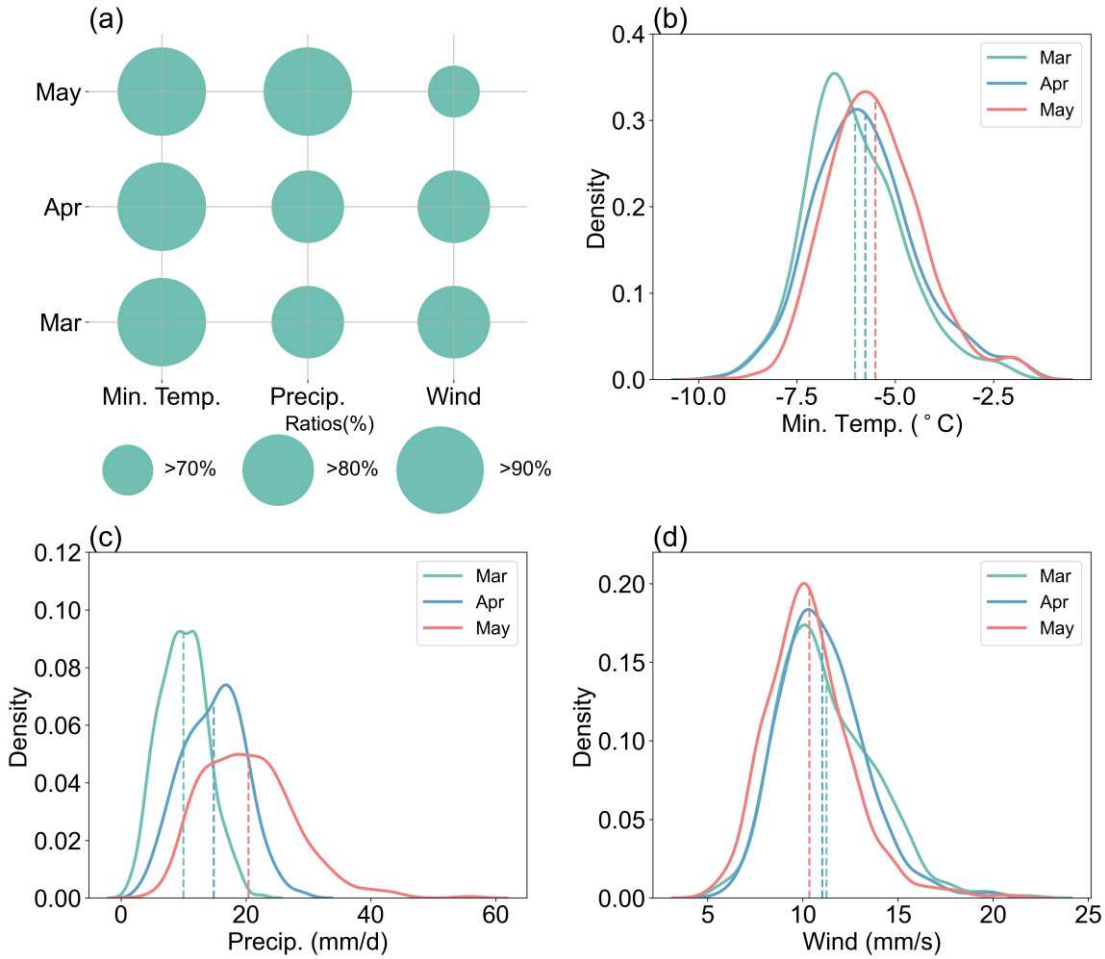

Figure 10 Monthly characteristics related to RCE. (a) The average frequency proportion of RCEs where the minimum temperature anomalies, precipitation and wind speed exceeded the corresponding thresholds during March–May in southern China, respectively. The threshold of the minimum temperature anomalies is less than 0°C, and the threshold of precipitation and wind speed is greater than 1mm/d and greater than 7 m/s. Probability density functions of monthly (b) minimum temperature anomalies, (c) precipitation and (d) wind speed related to RCE for 836 meteorological stations during March–May in southern China. The light green, light blue and light red dotted lines represent the average of 836 stations in March, April and May, respectively.

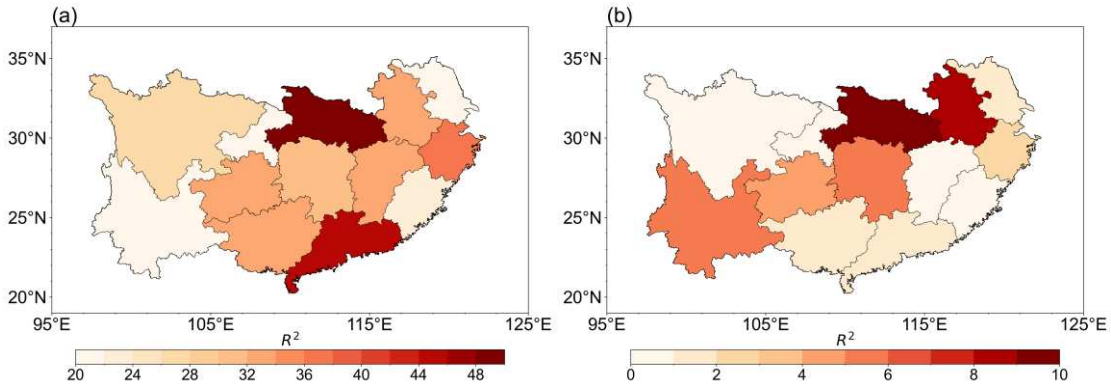

692

693 **Figure 11 Explanied varaition for rice yield anomalies.** (a) R^2 values of the full
694 statistical model accounting for mean climate conditions and climate variability. (b)
695 Difference in R^2 of full statistical model and reduced model, estimating the partial ex-
696 plained variance from spring climate variability. R^2 values are calculated from the ex-
697 plained variance of the multiple regression of rice yield anomalies aganist climate var-
698 iable anomalies.

699

700

Supplementary Materials

Decadal trend of spring rapid temperature variability and its impact on yield over southern China

Xianke Yang[1], Yixuan Zhang, Haosu Tang[3], Ping Huang[2], Xiaoxia Ling[1], Shaobing Peng[1], Dongliang Xiong[1,*]

1. MARA Key Laboratory of Crop Ecophysiology and Farming System in the Middle 9 Reaches of the Yangtze River, Huazhong Agricultural University, Wuhan, Hubei, 430070, 10 China

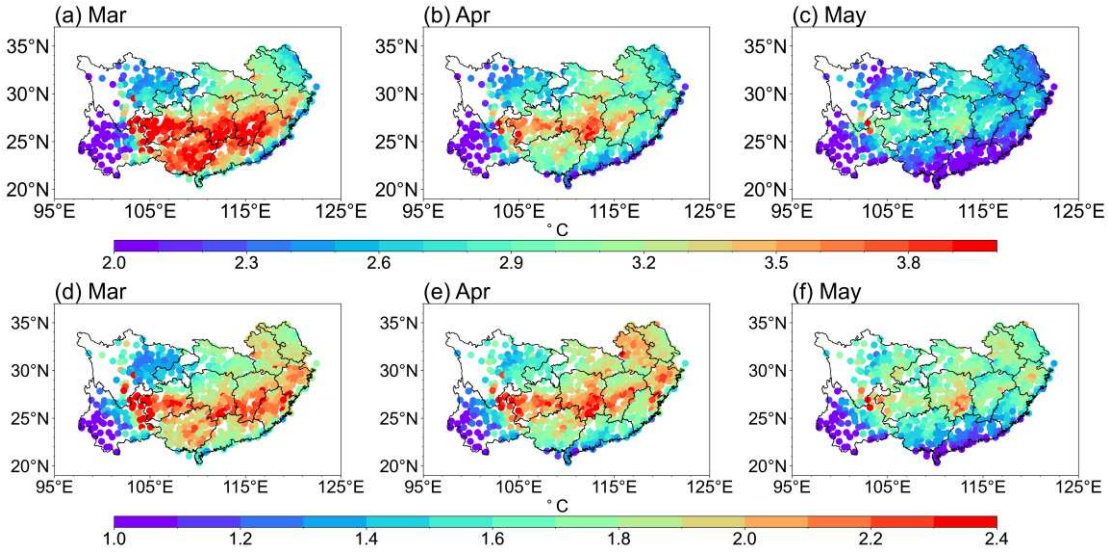

Figure S1. Spatial distributions of monthly means of (a–c) STD and (d–f) DTD during March–May from 1970 to 2022.

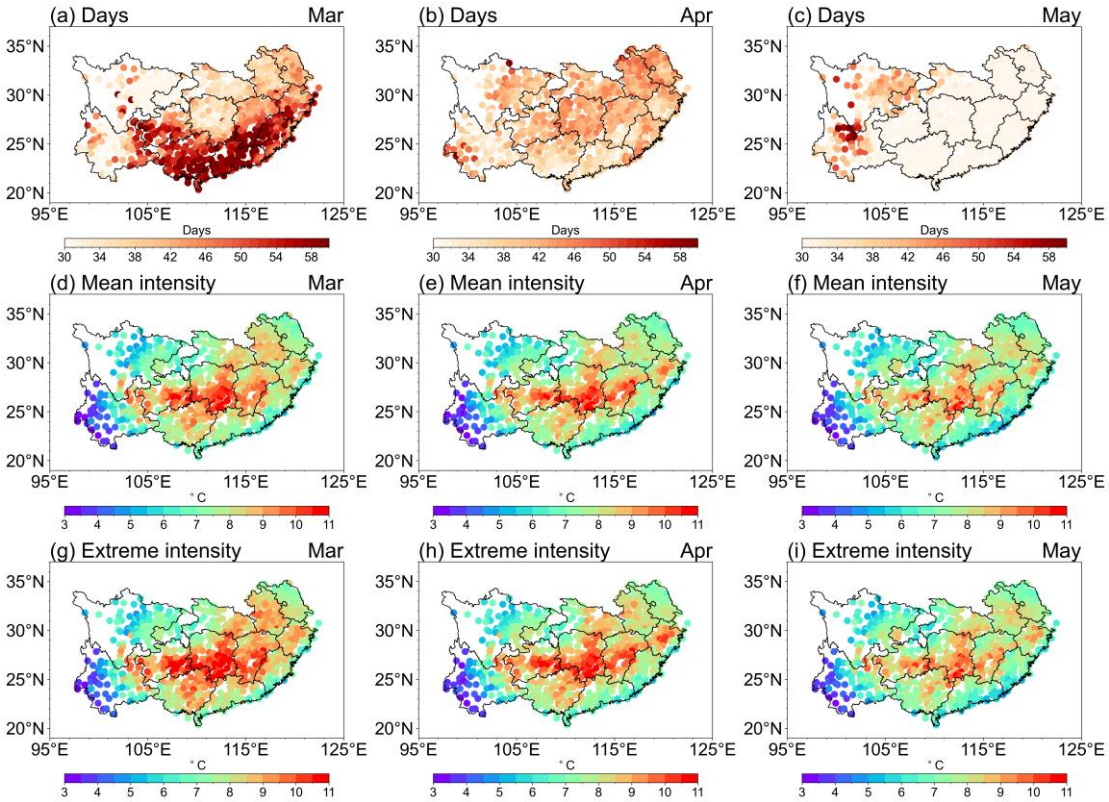

714

715 **Figure S2.** Spatial distributions of monthly means of (a–c) days, (d–f) mean intensity

716 and (g–i) extreme intensity of RCE during March–May from 1970 to 2022.

717

718

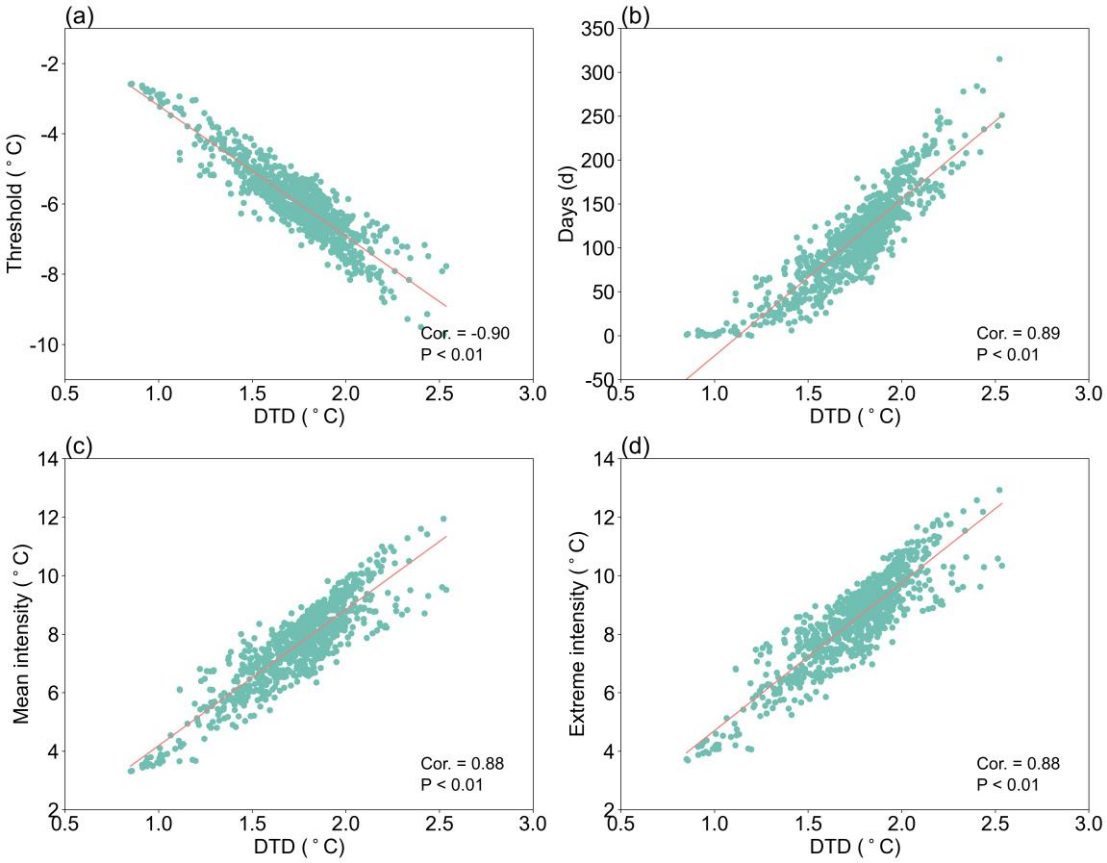

719

720 **Figure S3.** As in Figure 5, but for relationship between DTD and RCE.

721

722